X-ray absorption near-edge structure and extended x-ray absorption fine-structure investigation of Pd silicides

M. De Crescenzi
Dipartimento di Fisica, Universitá dell'Aquila, 57100 L'Aquila, Italy

E. Colavita*
Dipartimento di Fisica, Universitá della Calabria, 87036 Arcavacata di Rende, Cosenza, Italy

U. Del Pennino, P. Sassaroli, and S. Valeri
Dipartimento di Fisica, Universitá di Modena, 41100 Modena, Italy

C. Rinaldi, L. Sorba, and S. Nannarone
Dipartimento di Fisica, Universitá "La Sapienza," 00185 Roma, Italy
(Received 16 July 1984; revised manuscript received 27 March 1985)

X-ray absorption spectroscopy is used to investigate the near-L-edge structures of Pd in pure Pd and bulk Pd_2Si and PdSi silicides. Possible many-body effects are suggested to explain the apparent discrepancy between the occurrence of $L_{2,3}$ white lines and the $4d$ hole filling in Pd silicides. The interpretations of the extended fine structures and of the near-edge features are correlated with each other in order to find common support for a dynamical relaxation model for the $L_{2,3}$ deep core holes of Pd silicides.

I. INTRODUCTION

Technological interest[1] in metal-silicon compounds and their interfaces has stimulated a great deal of theoretical and experimental work in an effort to understand their physical and chemical properties.[1-5]

The present work gives new insight into the electronic and structural properties of Pd_2Si and PdSi. Detailed x-ray absorption measurements for Pd silicides in the near-edge (XANES)[6-10] and extended fine-structures (EXAFS)[11] regions above the $L_{2,3}$ and L_1 absorption threshold of Pd are discussed in terms of many-body effects. This interpretation complements and, in some respects, disagrees with previous ones on the same subject.[12,13]

It is generally accepted that x-ray edges of pure metals and their alloys can be described within the one-electron picture disregarding[6] any relaxation effect. The XANES spectra are thought to reproduce the l partial density of states (DOS) above the Fermi level (E_F).[8-10] Indeed, the disappearance of the sharp absorption peaks at the $L_{2,3}$ edges on going from near-noble to noble metals is one of the most important confirmations of the one-electron picture.[7] Within this framework the electronic structure of Pd silicides would suggest that absorption line shapes around the Pd $L_{2,3}$ edge would be very similar to those of noble metals. Both experimental[3,14] and theoretical[5] results report a narrowing as well as an energy lowering of d bands, with the consequence that a peaked density of empty d states is absent above E_F.

The present experimental results do not agree with the above expectations. Our findings, in fact, can be summarized as follows.

(i) We observe an energy shift of the Pd L core edge in Pd_2Si and PdSi with respect to pure Pd. In particular the $L_{2,3}$ edges are shifted toward higher energies of about 3 and 3.5 eV for Pd_2Si and PdSi, respectively. At the same time the L_1 edge is shifted by about 1 eV in the same direction.

(ii) The $L_{2,3}$ absorption line shape is asymmetric and its intensity increases with Si content in the Pd matrix. At the same time the $L_{2,3}$ branching ratio tends to the statistical value of the atomic configuration.

In order to explain the above results and to understand the mechanism responsible for the increase in absorption on going from Pd_2Si to PdSi we analyzed first the EXAFS region and we use then our findings to interpret the XANES line shapes. The two analyses complement each other and give electronic as well as structural information. In particular, important hints on the screening of the Pd $L_{2,3}$ core holes due to valence electrons in Pd silicides are obtained. The results of this procedure force us to invoke "excitonic" effects, which become stronger and stronger as the Si content in the Pd matrix increases: The higher the Si concentration, the more the Pd $L_{2,3}$ core holes are localized. The same mechanism of dynamical screening proposed by Mahan[15] and Nozieres and De Dominicis[16] (MND), is thus invoked to explain the origin of white lines in Pd silicides, in analogy to what occurs in alkaline metals.[17]

Similar effects (enhancement, asymmetry and energy shifts) have been recently observed by Mason[18] in the XANES spectra of Pd clusters where the Pd absorbing atom is thought to be in an atomiclike and unscreened enviornment. This could be considered a limiting case to which the present speculations can be extended.

Our results and interpretation disagree with those of Stöhr and Jaeger[12] and Rossi *et al.*[13] They, for example, do not observe the energy shift of Pd L core edge in Pd_2Si

and PdSi with respect to pure Pd and, moreover, do not support their conclusions through the complementary analysis of both XANES and EXAFS regions which has been crucial for discovering the occurrence of many body effects.

The paper is organized as follows: In Sec. II, the experimental details and the results are presented. Section III is devoted to the analysis and discussion of EXAFS and XANES data, while the conclusions are drawn in Sec. IV.

II. EXPERIMENTAL RESULTS

The experiments were performed at the x-ray beam line of the Frascati synchrotron radiation facility PULS (Progetto per la Utilizzazione della Luce di Sincrotrone). The storage ring ADONE was operated at an energy of 1.2 GeV and the typical electron current was 50 mA.

The incident radiation I_0, monochromatized by a channel-cut Si(220) crystal, was monitored by a gas ionization chamber. The intensity I transmitted through the sample was collected by a second chamber. Both chambers were filled with He and Ne gas at a pressure and at a concentration chosen to provide a 30% absorption for I_0 and a maximum absorption for I. The experimental apparatus and the data collection system used to perform x-ray absorption measurements have been described elsewhere.[19,20]

Pd_2Si and PdSi samples were prepared by heating a calibrated amount of Pd and Si powder in a vacuum of 10^{-10} Torr by an electron beam. The samples were characterized in bulk composition, homogeneity and long-range order by Rutherford backscattering and x-ray diffraction: Deviation from nominal stoichiometry was less than 1% and no trace of phases different than those studied, were detected. The diffraction patterns assured the high quality of the polycrystalline samples.

The Pd_2Si sample was then transferred in a UHV chamber for the surface analysis. The surface cleaning was achieved with a differential ion gun. An Ar^+ beam with energy between 0.5 and 5 keV and current density of about 10 $\mu A\,cm^{-2}$ was used over a rastered area of 3×3 mm^2. The changes of the relative Si-to-Pd concentration induced by the sputtering process were checked by analyzing the low-energy Si and Pd Auger lines with the elemental standard method. Taking into account backscattering factors and mean-free paths, it leads to the atomic concentration with an accuracy of $\pm2\%$. Details on this method can be found elsewhere.[21] No variations in the Si-to-Pd surface concentration with respect to the bulk were found for sputtering energy in the keV range.

A detailed analysis of the Si $L_{2,3}$ VV Auger line shape (Fig. 1) confirms the Pd_2Si character of the keV-sputtered surface. Although this line is qualitatively similar in the Pd_xSi ($x=2,3,4$) compounds,[22] the peak-to-peak intensity ratio of the c and d structures increases with x (inset of Fig. 1). The value obtained ($c/d=0.37$) implies $x=2$.

For the x-ray measurements the samples were prepared following a standard procedure. They were turned in form of powders which then have been sandwiched between two stripes of Kapton tape. Great care was taken to ensure uniformity over the sample areas exposed to the beam. All spectra were taken at room temperature. Fig-

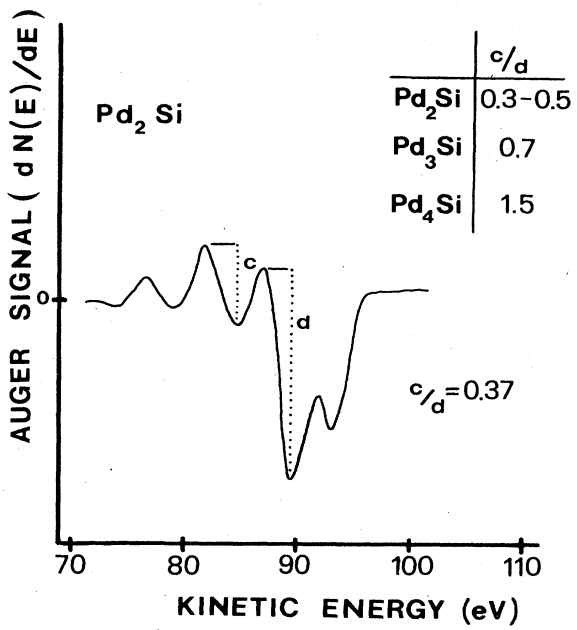

FIG. 1. Auger Si LVV spectrum of the Pd_2Si sample used for the x-ray absorption measurements. It was obtained after 5 keV Ar^+ sputtering. The intensity ratio of the Si c and d features is used as a calibration of the Pd concentration in the Pd-Si silicides (Refs. 21 and 22).

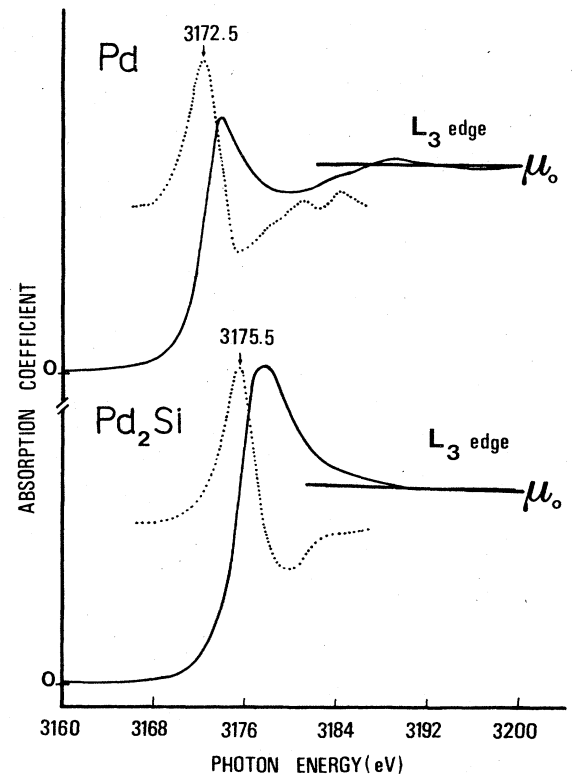

FIG. 2. L_3 absorption edge of Pd in Pd metal (upper curve) and in Pd_2Si (lower curve). The dotted lines show the first derivative of the XANES spectra. The atomic absorption μ_0 coefficients utilized for analyzing the EXAFS oscillations and the white lines intensities, are also shown.

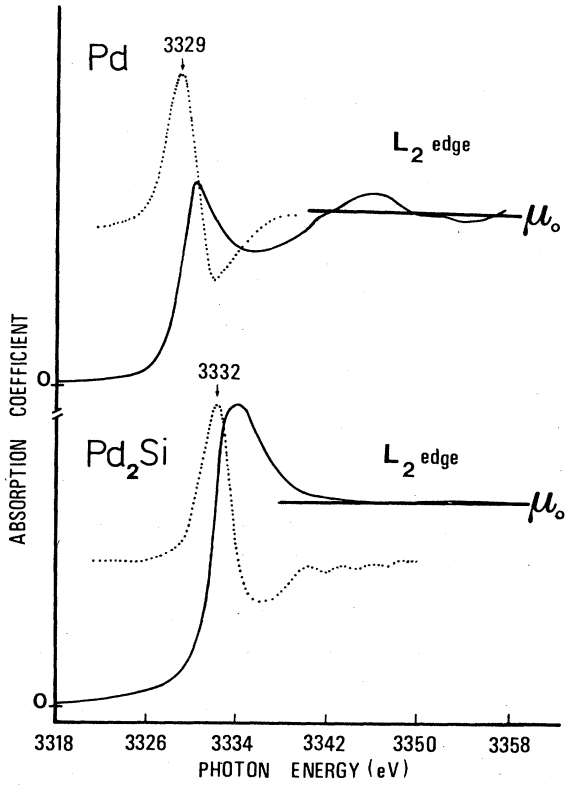

FIG. 3. L_2 absorption edge of Pd in Pd metal (upper curve) and in Pd_2Si (lower curve). The dotted lines show the first derivative of the XANES spectra. The atomic absorption μ_0 coefficients utilized for analyzing the EXAFS oscillations and the white lines intensities are also shown.

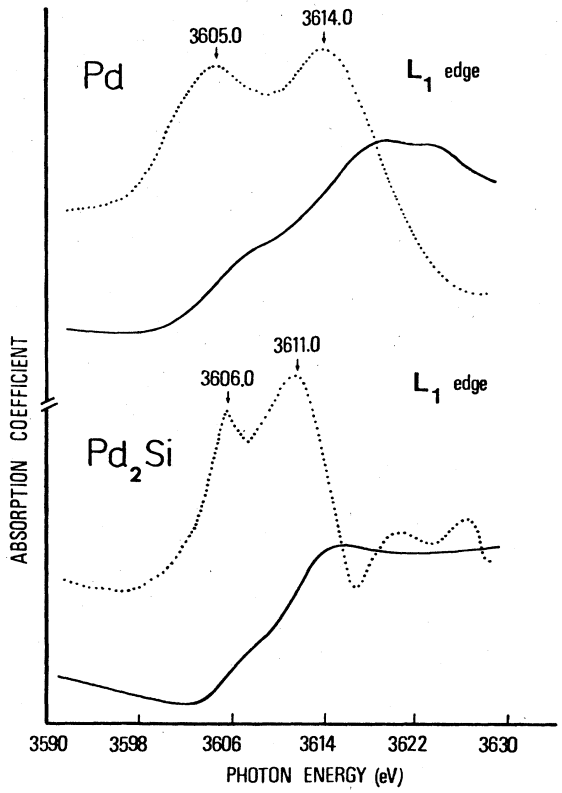

FIG. 4. L_1 absorption edge of Pd in Pd metal (upper curve) and in Pd_2Si (lower curve). The dotted lines show the first derivative of the XANES spectra.

ures 2, 3, and 4 show the x-ray absorption near-edge structures of Pd and Pd_2Si in the region of Pd L_3, Pd L_2, and Pd L_1 shell excitations. The line shapes of x-ray absorption coefficient show evident and important differences on going from Pd to Pd_2Si. Their intensities increase with respect to the atomic absorption coefficient μ_0, the line shapes become rounded and a well-developed asymmetry is present in the Pd_2Si system. Moreover the energy threshold is shifted toward higher binding energies of about 3 eV. The PdSi L edges, which show an overall similarity with the Pd_2Si ones, are characterized by a higher energy shift (0.4 eV) and a higher increase in intensity.

Figure 5 shows the L_2 and L_1 EXAFS $\chi(k)$ of pure Pd and their relative radial distribution functions $F(R)$ obtained by a Fourier transform according to the standard EXAFS analysis.[11] Figures 6 and 7, instead, present the EXAFS oscillations above the L edges of Pd in Pd_2Si and their relative $F(R)$'s.

III. DISCUSSION

A. EXAFS analysis

The interpretation of EXAFS spectra around the L_1 and $L_{2,3}$ edges has been carried out by using the theoretical $\chi(k)$ function written in the single scattering approximation, and given by[23,24]

$$\chi(k)=\frac{\mu-\mu_0}{\mu_0}=\sum_J A_J(k)\sin[2kR_J+\phi_J(k)] , \quad (1)$$

where μ_0 and μ are the atomic and total absorption coefficient, respectively. The $A_j(k)$ term can be written as

$$A_J(k)=\frac{N_J f(k,\pi)}{kR_J^2}S_0^2 e^{-2\sigma_J^2 k^2} e^{-2R_j/\lambda(k)} , \quad (2)$$

where N_j is the number of backscatters of type j located at the distance R_j from the absorbing atom, $f_j(k,\pi)$ is the backscattering amplitude, $\exp(-2\sigma_J^2 k^2)$ is the Debye-Waller factor taking into account both thermal fluctuations and static disorder. $\exp[-2R_j/\lambda(k)]$ is a term accounting for the inelastic scattering and S_0^2 is the attenuation due to many body effects.[25] The photoelectron wave vector k is defined by $k=(2m/\hbar^2)^{1/2}(\hbar\omega-E_0)^{1/2}$, where E_0 and $\hbar\omega$ are the threshold and photon energies, respectively. As is well known,[24] the total phase shift $\phi_j(k)$ of the photoelectron wave depends on the absorbing (A) as well as on the backscattering atom (B). Thus for K and L_1 edges, it occurs:

$$\phi_J(k)=\phi_A^l(k)+\phi_B(k)-\pi , \quad l=1 \quad (3)$$

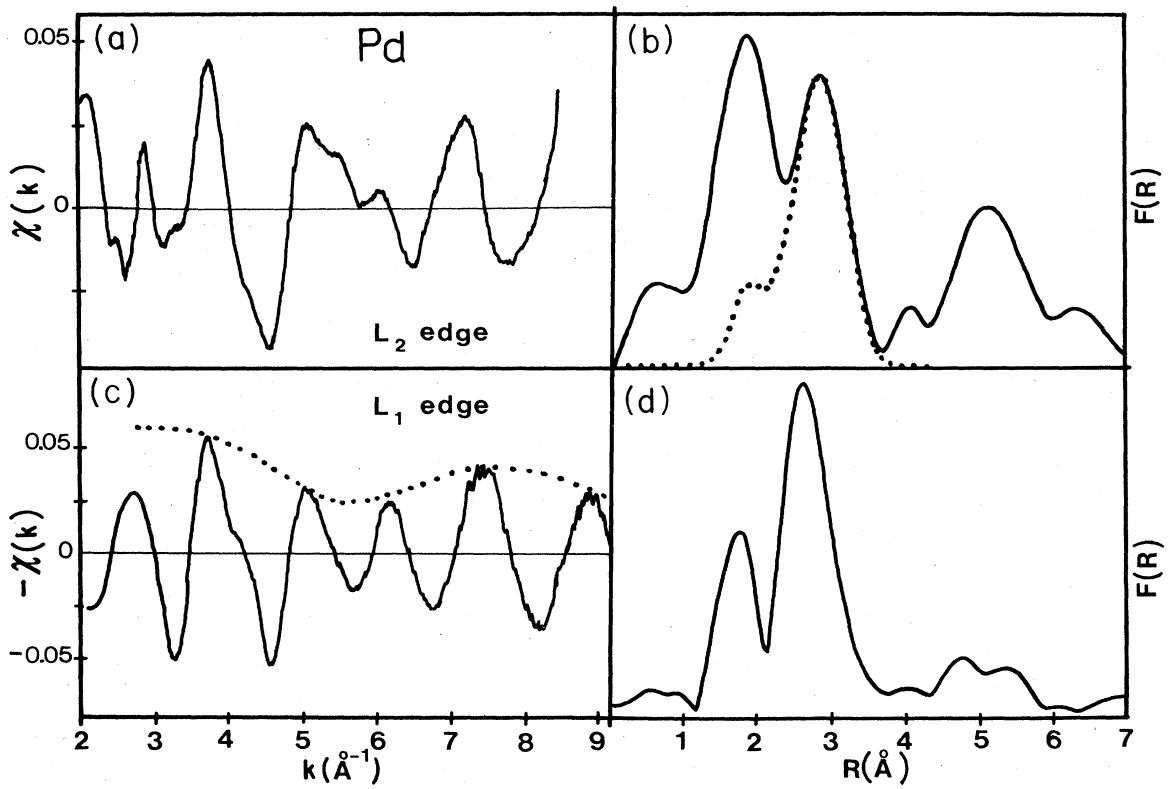

FIG. 5. EXAFS modulation $\chi(k)$ for Pd in Pd metal around L_2 (a) and L_1 (c) edges. (b) and (d) show their Fourier transforms, respectively. The dotted line in (b) is the $F(R)$ as obtained from the EXAFS formula [Eq. (1)] using the first Pd-Pd shell. The backscattering amplitude and phase shifts of Teo and Lee (Ref. 24) (Fig. 8) have been used. The dotted line in (c) is the experimental backscattering amplitude obtained by Fourier filtering of the first shell of panel (d). Note the reversed sign between L_2 and L_1 EXAFS oscillations due to the π difference in the phase shift (Fig. 8).

while for $L_{2,3}$ edges,

$$\phi_J(k)=\phi_A^l(k)+\phi_B(k)\ ,\quad l=2,0\ . \tag{4}$$

Electric dipole selection rules allow transitions from the $L_{2,3}$ core levels into conduction states having both $s\,(l=0)$ and $d\,(l=2)$ partial wave character. However it has been demonstrated[26] that the s partial wave contribution in the L_3 (and L_2) spectra can be neglected because the $p\rightarrow\epsilon s$ matrix element is much smaller than the $p\rightarrow\epsilon d$ term.

We present first the analysis of the L_1 EXAFS of Pd since it gives a better understanding of the observed structures,[27] and it is helpful as term of comparison, for interpreting the radial distribution function $F(R)$ of Pd silicides.

The first structure of $F(R)$ at 1.7 Å [Fig. 5(d)] is due to the Ramsawer-Townsend modulation of the backscattering amplitude,[24] while the main peak at 2.58 ± 0.02 Å is due to the presence of the twelve first neighbors atoms of the fcc lattice around the central atom. It corresponds to the crystallographic value of $R_j=2.76$ Å to which it moves after the correction[24] [Eq. (3)] for the phase shift. Further insights into the properties of the $\chi(k)$ of Pd L_1 edge come directly from the experimental backscattering function obtained by back Fourier filtering of the $F(R)$ between 1 and 3.5 Å. The minimum of the backscattering amplitude function [Fig. 5(c) dotted line] reproduces the modulation of the $\chi(k)$ signal as expected.

The $F(R)$ function, obtained from the L_2 signal, presents an overall similarity with the above result but it is different in some features. The first peak, for example, is affected by the presence of the superposition between L_3 and L_2 oscillations. The comparison between theoretical and experimental $L_2-F(R)$ is reported in Fig. 5(b) to give a measure of this effect. Notice that the $L_1-\chi(k)$ has been reversed in order to make easier a one-to-one correspondence with the $L_2-\chi(k)$ following the procedure[26] already used for Au.

As in the case of Pd, the Pd silicides exhibit similar L_3, L_2, and L_1 EXAFS-Fourier transforms (Figs. 6 and 7). Contrary to Pd metal, however, the EXAFS oscillations in the silicides are basically built from a single $\sin(2kR)$ function and *do not* change sign on going from $L_{2,3}$ to L_1 edge. This finding is quite uncommon and deserves to be stressed since it may point to a limitation in the one-electron description of EXAFS structures. In the case of L x-ray absorption spectra of rare-earth metals,[28] for example, the single-particle picture of the L_1 line shape as well as of the $L_{2,3}$ white lines is assessed[29] and the peaks in the L_3 EXAFS spectrum are associated with valleys in the L_1 EXAFS spectrum. This corresponds to a phase shift of π between the s to p (L_1) and p to d ($L_{2,3}$) terms. Indeed, electric dipole selection rules allow transitions

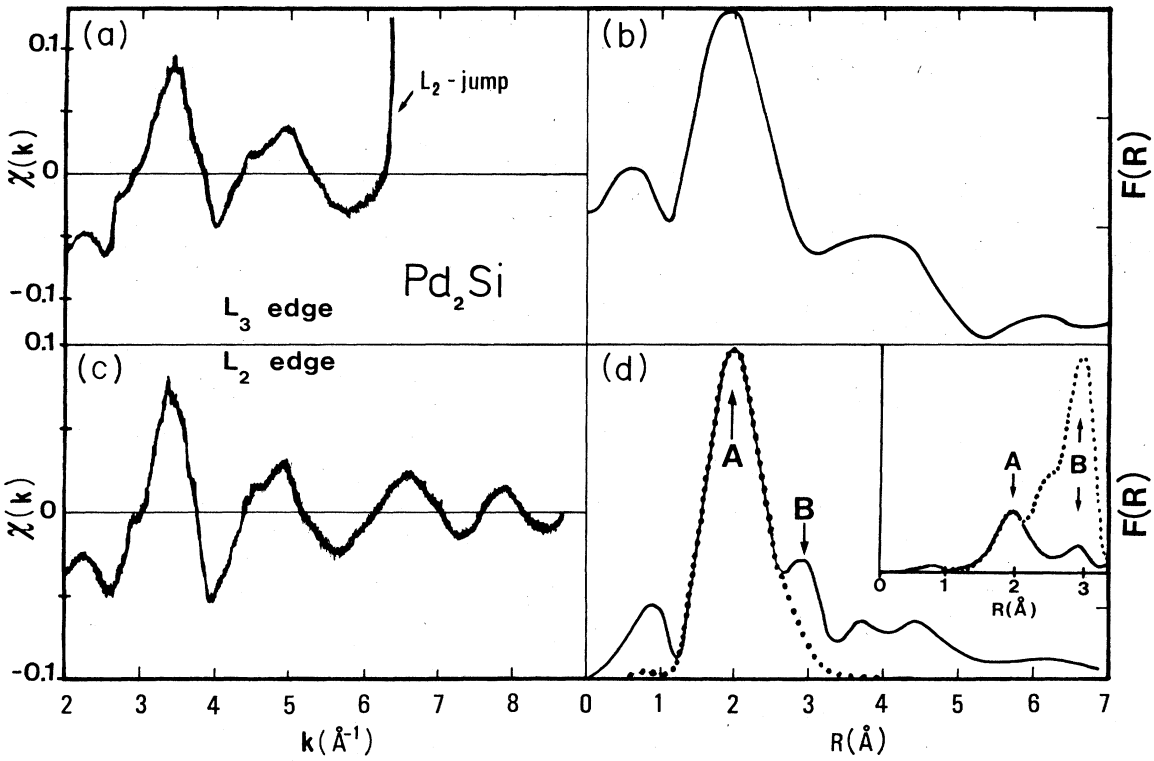

FIG. 6. EXAFS modulation $\chi(k)$ for Pd in Pd_2Si around L_3 (a) and L_2 (c) edges. (b) and (d) show their Fourier transforms, respectively (full lines). For the L_3 edge the interpretation was performed up to $k_{max}=6.5$ Å^{-1} due to the L_2 edge jump. The dotted line in (d) shows the computed Fourier transform obtained using the lattice parameters of Pd-Si pairs first nearest neighbors (Fig. 9). The Si backscattering amplitude and the Pd-Si phase shift ($p \rightarrow d$) of Teo and Lee (Ref. 24) (Fig. 8) have been used. The fit is good in R space but in k space there is a nearly constant π shift between theory and experiment (see text). The inset of (d) shows the same EXAFS model with the inclusion of the Pd-Pd first coordination shells (Fig. 9).

from the $2p$ core levels into conduction states having both s and d partial wave character, but the s partial-wave contribution in the L_3 spectra is usually ignored because of the much smaller $2p \rightarrow \epsilon s$ matrix element compared with the $2p \rightarrow \epsilon d$. Thus, what is the significance to be attached to the correspondence between *peaks* in L_3 and *peaks* in L_1 EXAFS spectra of Pd in Pd silicides? Might $2p \rightarrow \epsilon s$ transitions be more predominant in Pd silicides than in Pd itself or, more in general, than in transition and rare-earth metals?

We will focus on the L_2 EXAFS $F(R)$ rather than on the L_3 EXAFS $F(R)$ because of the wider k integration range. The first peak [A in Fig. 6(d)] at 1.96 ± 0.02 Å is due to the first-nearest-neighbor cage of silicon, while the second peak [B in Fig. 6(d)] at 2.90 ± 0.02 Å is due to Pd atoms. These assignments are made on the basis of a comparison between the experimental and the computed $F(R)$ [Fig. 6(d) inset]. The phases and the backscattering amplitudes have been taken from Ref. 24 (see Fig. 8), while the structure parameters of Pd_2Si have been taken from Ref. 30 (see Fig. 9). Of course, the complex crystal structure of Pd_2Si with inequivalent Pd atoms has been taken into account in the computed $F(R)$ model.[31]

Although the relative intensity of the A and B structures [Fig. 6(d) inset] is not reproduced, they occur in the real space where the experimental findings are. A closer agreement has been found by using only Pd-Si pairs [dotted line in Fig. 6(d)]. Also, reproducing the peak B, we were forced to decrease the S_0^2 factor of the EXAFS formula [Eq. (1)] from 0.7, found for pure Pd, to 0.2. No attempt was successful by adjusting only the Debye-Waller parameters σ^2 (Pd-Pd) and σ^2 (Pd-Si) and taking $S_0^2=0.7$. In brief, the calculated and the experimental $F(R)$ of Pd_2Si are similar for the number of the main structures and for their position in the real space but are very different for their relative intensity. Since any simulation of disorder by using large and different Debye-Waller factors (up to $\sigma_I^2=0.03$ Å^{-2}; $\sigma_{II}^2=0.035$ Å^{-2}) for the two inequivalent Pd sites, was ineffective to reproduce the experimental $F(R)$, we were forced to adjust the S_0^2 factor. This fitting parameter is quite small[32] with respect to that for pure Pd, nevertheless, such a large difference can be taken, at this stage of art, as the indication that relaxation effects on the Pd central atom in Pd_2Si are present, regardless of the absolute value of S_0^2. All that provides another hint that the one-electron picture is not completely adequate in describing the Pd_2Si system.

It is well known,[25] in fact, that one-electron calculations overestimate scattering amplitudes unless a correction is made for the relaxation of passive electron orbitals.

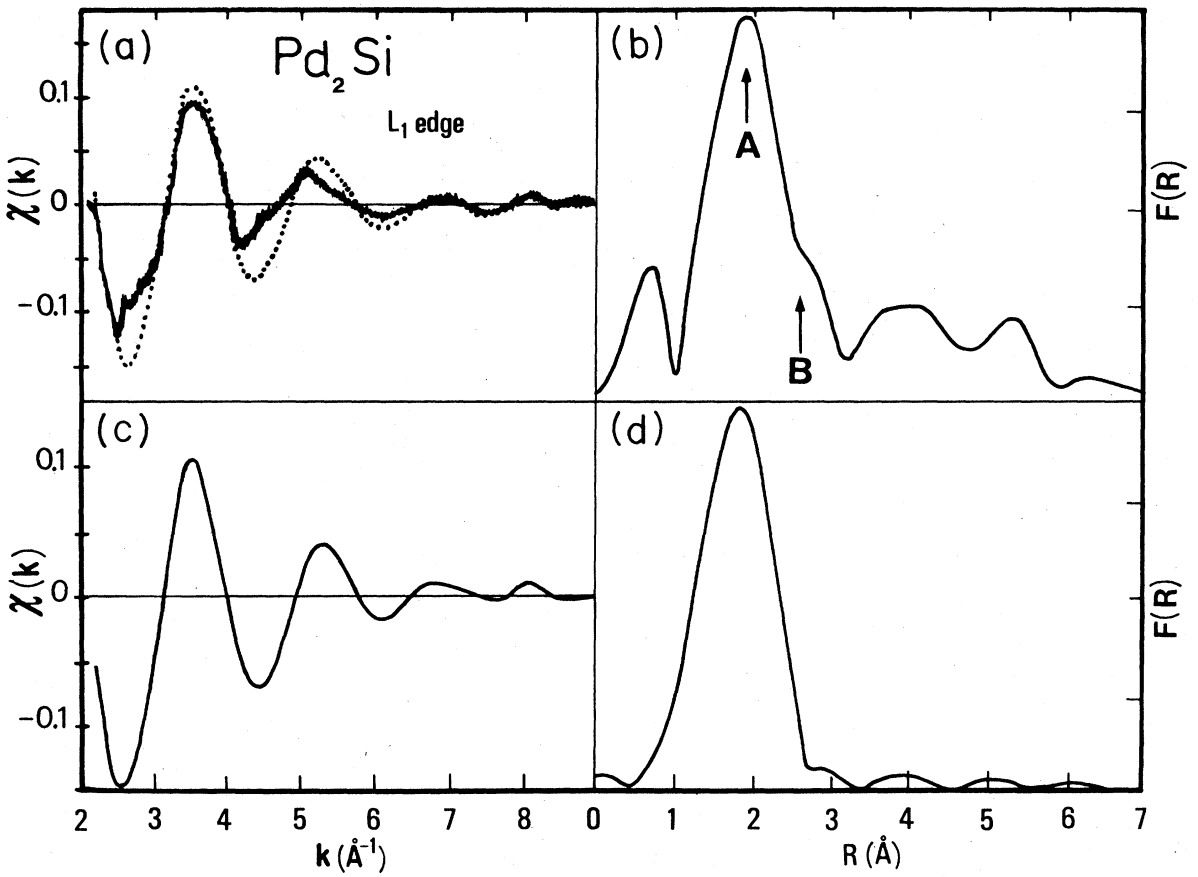

FIG. 7. (a) EXAFS oscillations $\chi(k)$ for Pd L_1 edge in Pd_2Si. (b) Its Fourier transform. The dotted line in (a) shows the back Fourier inversion of the A peak. (c) EXAFS model [Eq. (1)] computed using the pair Pd-Si nearest neighbors (Fig. 9). The Si backscattering amplitude and the Pd-Si L_1 phase shift (Fig. 8) are taken from Teo and Lee (Ref. 24). (d) Fourier transform of the theoretical EXAFS model.

Namely, single-particle matrix elements have to be scaled by a reduction factor $S_0^2 = |\langle \psi'_{N-1} | \psi_{N-1} \rangle|^2$, where $|\psi'_{N-1}\rangle$ and $|\psi_{N-1}\rangle$ are the wave functions of the $N-1$ electrons with and without the core hole, respectively.

In the case of the L_1 edge of Pd in Pd silicides, the radial distribution function can be interpreted as for the $L_{2,3}$ edges. The back Fourier transform of the peak A [Fig. 7(b)] shows a backscattering amplitude similar to that of Si [Fig. 8(a)], supporting the assignment that the first Si neighbor shell gives the main contribution to the EXAFS signal and moreover the above analysis procedure.

The experimental phase shifts are compared in Fig. 10 with the theoretical ones[24] computed for Pd-Si pairs. The continuous lines are the Teo and Lee phase shifts[24] for the $L_1(s-p)$, $L_{2,3}(p-s)$, and $L_{2,3}(p-d)$ transitions, while the dotted and triangular lines are the experimental L_1 and $L_{2,3}$ phase shifts, respectively. While the theoretical and experimental L_1 phase shifts are quite similar, for the $L_{2,3}$ edges, the phase shifts show noticeable differences. At low k values, the $L_{2,3}$ experimental phase shift looks like the $L_{2,3}(p-s)$ term while at higher k values tends toward the $L_{2,3}(p-d)$ term. It is worthwhile to note that this behavior is in concomitance and very likely related to the absence of the π phase shift in the $\chi(k)$ on going from the L_1 to the $L_{2,3}$ edge of Pd in Pd_2Si, as instead expected on the basis of Eqs. (3) and (4) when only the $p-d$ term is used (see the case of pure Pd, Fig. 5). Thus, the experimental results suggest, once more, that the theoretical approximations used for calculating the phase shifts[24] are quite good for the Pd L_1 excitation in Pd silicides but are not applicable to the Pd $L_{2,3}$ excitation.

Noguera and Spanjaard[33] have shown that the occurrence of relaxation effects due to the creation of a deep hole in a simple metal can modify the k dependence of the phase shift as calculated in the "equivalent core approximation."[34] Indeed the hypothesis of a dynamic screening gives rise to a phase-shift intermediate between the two curves which correspond to the no-screening and static screening, respectively, of the central atom. It could be interesting to apply the same theory to Pd silicides in order to find out the amount and the kind of the many body interaction taking place after the creation of Pd $L_{2,3}$ holes. Certainly, the experimental behavior of the phase

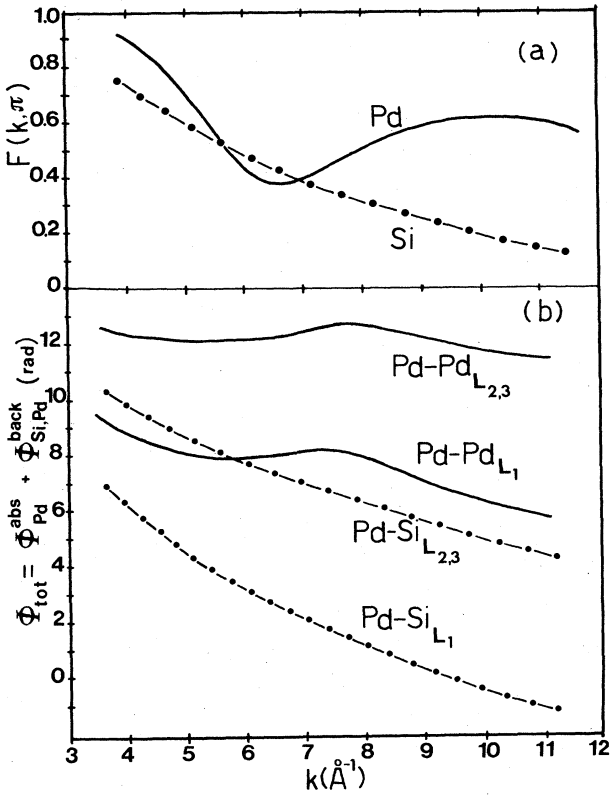

FIG. 8. (a) Backscattering amplitude for Pd and Si as reported by Teo and Lee (Ref. 24); (b) phase shifts calculation of Pd-Pd and Pd-Si pairs for L_1 ($s \rightarrow p$ transitions) and $L_{2,3}$ ($p \rightarrow d$ transitions) edges.

shift is indicative of mechanisms which cannot be explained within the equivalent core approximation. These findings assign an important role to the core-hole interaction which has been completely disregarded in previous interpretations.[12,13]

B. Near-edge region

The shape of the x-ray absorption coefficient of *d* metals is generally a picture of the density of empty states above E_F.[6–10,35] The behavior of the absorption coefficient of Pd *L* edges is, in fact, well reproduced in the one electron theory as shown in Fig. 11, where the theoretical results of Müller and Wilkins[8] and Smulowicz and Pease[9] and the present experimental results are compared. The white line intensity is due to the presence of a sharp peak in the *d* empty final states at the Fermi level. On going to the next noble metal, their disappearance is expected and observed.

Within the single-particle frame, a noble metal-like behavior is expected for Si *d* metal compounds. The electronic structure of metal silicides is in fact well understood in terms of Si 3*p* and Pd 4*d* hybrid bonding states (at about 5 eV below E_F) and partially occupied antibonding states close to the Fermi level.[5] As shown by the calculations of Bisi and Calandra[5] reported in Fig. 12, the density of empty *d* states at E_F of Pd_2Si is *neither high nor peaked.*[36] Thus the intensity of $L_{2,3}$ white lines of pure Pd, due mainly to dipole allowed $p-d$ transitions, is expected to be strongly reduced in Pd silicides. On the

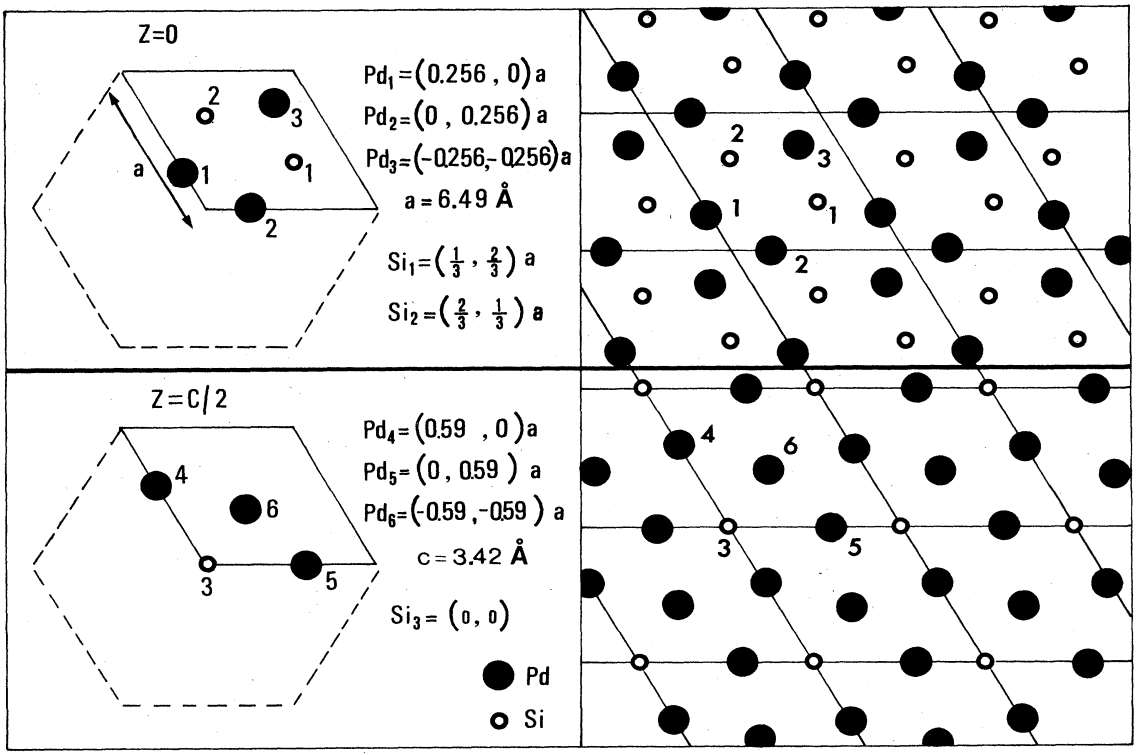

FIG. 9. Structural lattice parameters of Pd_2Si for the $z=0$ and the $z=c/2$ planes (Refs. 5 and 28).

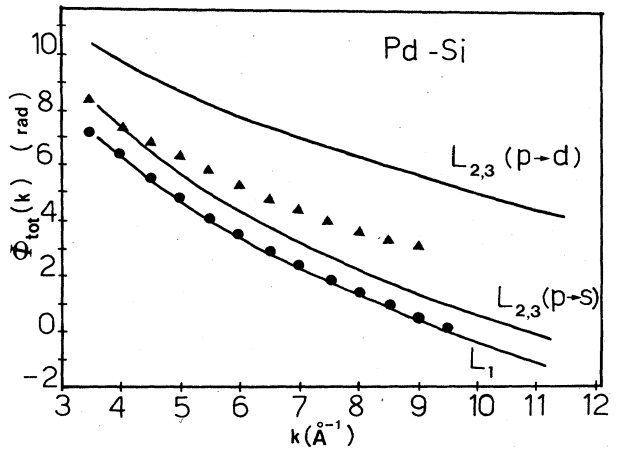

FIG. 10. ● represents L_1 experimental Pd-Si phase shift obtained from the Pd_2Si $F(R)$ (Fig. 7). It is compared with the L_1 theoretical phase shift of Teo and Lee (Ref. 24). ▲ represents L_2 experimental Pd-Si phase shift obtained from the Pd_2Si $F(R)$ (Fig. 6). It is compared with the $L_{2,3}$ theoretical phase shift (Ref. 24). The $p \rightarrow s$ and $p \rightarrow d$ phase-shift terms are reported.

contrary, the x-ray experiments (Figs. 1 and 2 and Ref. 13) show an intensity increase on going from pure Pd to Pd_2Si and PdSi.

This kind of phenomenology is common to a number of other systems which are all characterized by a bonding and an environment similar to that of Pd in Pd silicides. PdSi metallic glasses,[37] transition metal-metalloid alloys,[38] Pd-oxide,[39] and Pd metallic clusters[18] all show a steep increase at the Pd $L_{2,3}$ edges. At the same time a wide variety of experimental techniques such as photoemission,[2,14] magnetic susceptibility[40,41] and specific heat measurements[42] indicate a low value of the partial d density of empty states at E_F.

Pease *et al.*[37] proposed a lifetime broadening effect to settle the conflict between the intensity increase of near L edges structures and the evident filling of Pd d empty states. This has been proposed to explain the occurrence of white lines in Pd-Si metallic glasses. Since the core-hole broadening is so much greater than the width of the unoccupied d band, they predict that the shape of $L_{2,3}$ white lines is sensitive to the integrated number of $4d$ holes and not solely to the density of empty d states at E_F.

Although it might be tempting to stay within the band-structure framework, we will interpret the $L_{2,3}$ white lines in Pd silicides as due mainly to many body effects[15–17] in analogy with free-electron alkaline metals.

Correlation and localization between the excited electron and the core hole mediated by the screening of conduction electrons have been suggested to explain the high intensity of $L_{2,3}$ edges observed in alkaline metals in spite of the absence of d empty final states. The theoretical formulation by Mahan[15] and Nozieres and De Dominicis[16] (MND), leads to an expression for the x-ray absorption coefficient $\mu(w)$ given by

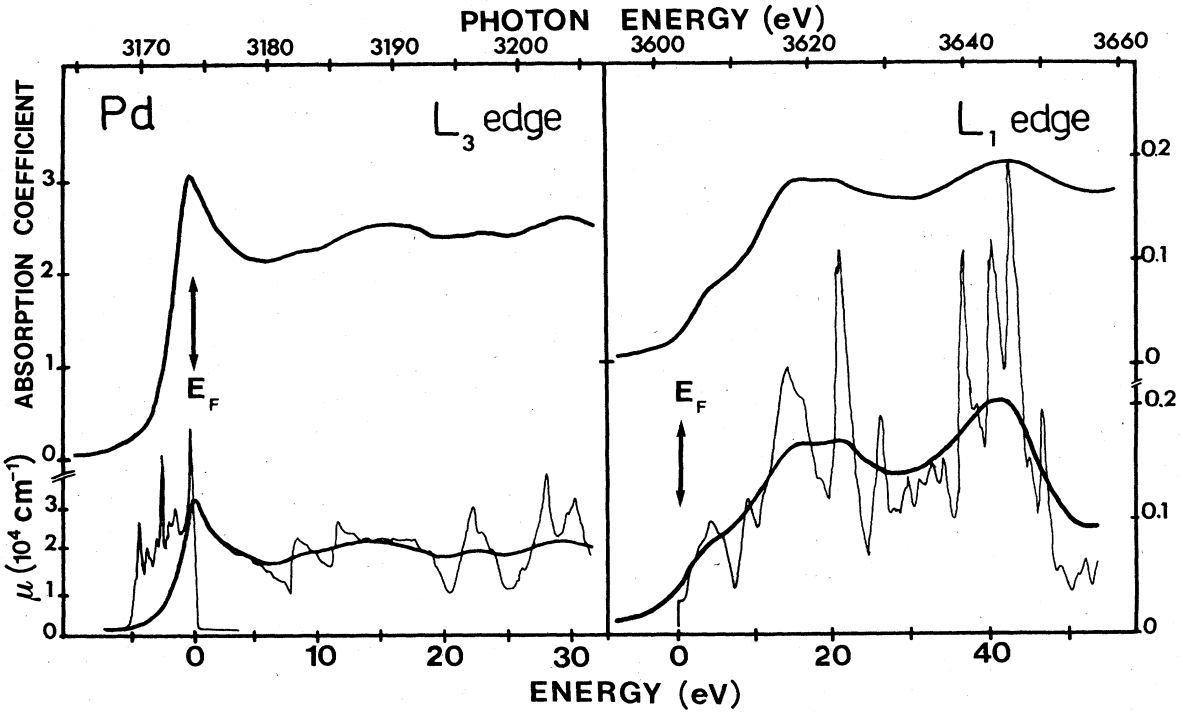

FIG. 11. Experimental L_3 and L_1 XANES region for Pd metal (upper curves). The lower curves show the computed partial L_3 and L_1 density of states (thin lines) and the broadened spectra (thick lines) as reported by Müller and Wilkins (Ref. 8). The energy origin is at the Fermi level.

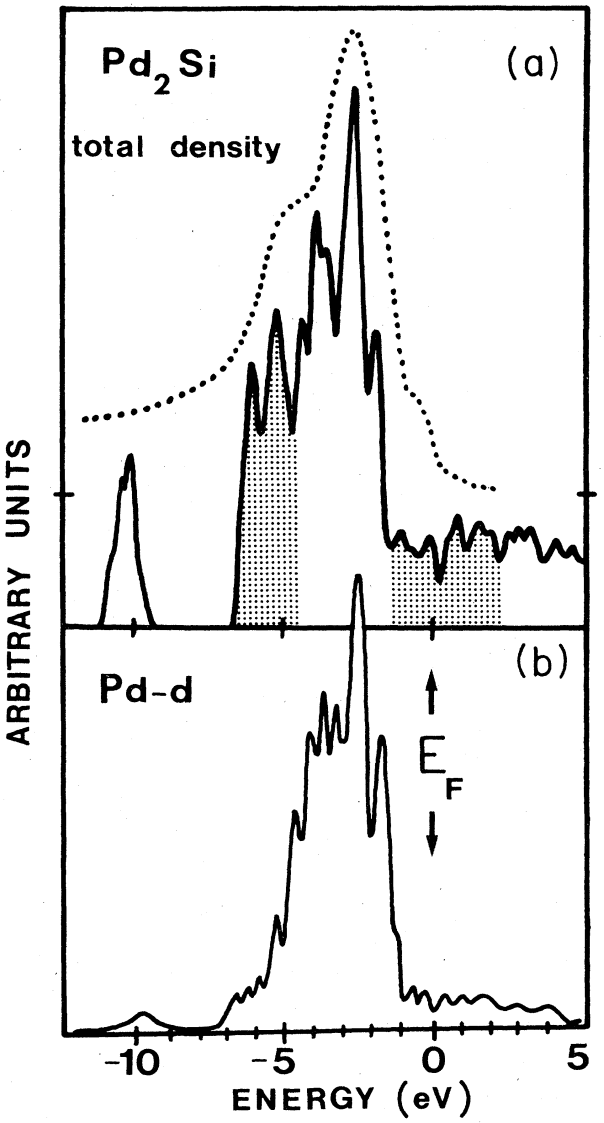

FIG. 12. (a) Total Pd_2Si density of states computed by Bisi and Calandra (Ref. 5). The shaded areas indicate $p-d$ bonding and antibonding states. The dotted line is the photoemission spectrum (Refs. 3 and 14), which reproduces the theoretical features. (b) Pd d contribution (Ref. 5) to the total density of states.

$$\mu(\omega)=|A_{l=0}(\omega)|^2\left[\frac{\Sigma_0}{\omega-\omega_0}\right]^{\alpha_0}+|A_{l=2}(\omega)|^2\left[\frac{\Sigma_0}{\omega-\omega_0}\right]^{\alpha_2}, \quad (5)$$

where $|A_l(\omega)|^2$ is the usual one electron-dipole transition probability with l final-state symmetry, ω_0 is the threshold energy and Σ_0 is a characteristic energy parameter of the order of the conduction-band width. The exponents α_0 and α_2 define the contribution of each channel to the optical absorption. The enchancement of $\mu(\omega)$ at ω_0 is due to the prevalence of the $p-s$ over the $p-d$ channel.

The analogy between the phenomenology of alkaline metals and Pd silicides is supported by a number of observations. We find (i) an energy shift of Pd L core edges in Pd_2Si and PdSi with respect to pure Pd; (ii) white lines, in spite of a low density of empty d states at E_F; (iii) an asymmetric absorption line shape; (iv) the occurrence of dynamical screening mechanisms around the Pd atom involving s final states as suggested by the EXAFS analysis.

In Fig. 13 the x-ray absorption coefficient calculated

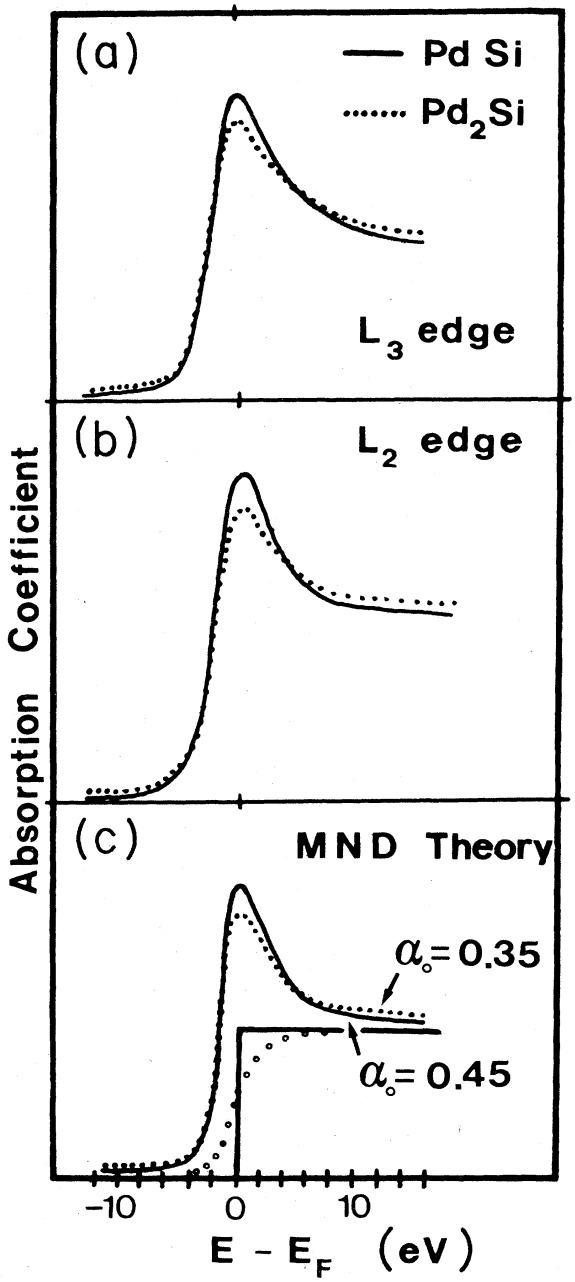

FIG. 13. L_3 (a) and L_2 (b) near-edge regions for Pd in Pd_2Si (dotted lines) and PdSi (solid lines). (c) $L_{2,3}$ absorption edge obtained from Eq. (5) according to Mahan-Nozieres and De Dominicis theory (Refs. 15 and 16). Only the $p\rightarrow s$ transitions have been considered. The values $\alpha_0=0.35$ (dotted line) and $\alpha_0=0.45$ (solid line) are used. The arctan function (open dotted line) which reproduces the $L_{2,3}$ step jump, has been broadened ($\Gamma=0.5$ eV).

according to the MND theory[15,16] is compared with the present results. The experimental line shape can be reproduced by using only the α_0 exponent which is an indication of $p-s$ optical transitions.[43] Since α_0 increases on going from Pd_2Si to PdSi the amount of s final states at E_F is expected to increase as a function of the Si concentration. This suggests again a dynamical screening and a localization of $L_{2,3}$ Pd core holes induced by the Si first-neighbor's shell. The evolution of the $L_{2,3}$ branching ratio also supports the view of an atomic environment built up around each Pd site as the Si content increases. The examples of Pd clusters[18] and of Pd embedded in liquid crystals,[44] where an enhancement, an asymmetric shape, an almost atomic branching ratio and an energy shift of the $L_{2,3}$ absorption coefficient is observed, makes us confident that atomic-like effects take place in Pd silicides.

As a final point, we mention that while the L_1 phase shift, does not show any anomolous k-dependence and is in good agreement with Teo and Lee calculations, the near-edge region of the L_1 absorption coefficient reproduces the p partial density of empty states within the one-electron picture.

IV. CONCLUSIONS

The joint analysis of EXAFS and XANES of Pd L edges in Pd silicides reveals the occurrence of many-body effects. The resulting picture of Pd_2Si and PdSi systems consists of a Pd atom in an atomiclike bonding environment. The $L_{2,3}$ hole localization is mainly responsible for the asymmetry and intensity of the absorption coefficient on going from pure Pd to PdSi. The one-electron model is in fact unable to reproduce the $L_{2,3}$ white lines of Pd in Pd silicides, and a mechanism similar to that proposed by MND for explaining the edge singularities of alkaline metals is suggested.

This interpretation disagrees with previous models but our EXAFS and XANES results, especially the energy shift, the asymmetry of $L_{2,3}$ white lines and the anomolous k dependence of $L_{2,3}$ phase shift, do indicate the occurrence of dynamical screening effects.

Although our EXAFS and XANES investigations are self-consistent and are supported by literature results on similar systems, only detailed theoretical calculations could allow the passage from a qualitative to a quantitative model and clarify the role of $L_{2,3}$ core holes in the XANES line shapes of Pd silicides.[45] An analogous study for $NiSi_2$ around the $L_{2,3}$ core edges of Ni could confirm the present interpretation, since the localization of $L_{2,3}$ holes in $NiSi_2$ relative to the metal should be even more evident. Moreover, investigation of different core levels could point out the dependence of the above mechanism on the deep core-hole symmetry. In any case the present procedure claims caution in interpreting surface EXAFS data[12,46] of nonstoichiometric surface compounds when bulk silicides phase shifts are used.

ACKNOWLEDGMENTS

We are particularly indebted to C. Calandra for many helpful discussions, suggestions, and a critical reading of the manuscript. The help of the staff of the Frascati Synchrotron Radiation Laboratories where the x-ray absorption measurements were performed is greatly appreciated and acknowledged. One of us (M.D.C.) wishes to thank A. Balzarotti for useful discussions. This work was supported by the Gruppo Nazionale di Struttura della Materia, Consiglio Nazionale delle Ricerche.

*Present address: Department of Physics, University of Wisconsin-Madison, Madison, WI 53706.

[1]G. W. Rubloff, Surf. Sci. **132**, 268 (1983), and references therein; L. J. Brillson, Surf. Sci. Rep. **2**, 123 (1982).

[2]G. Rossi, I. Lindau, L. Braicovich, and I. Abbati, Phys. Rev. B **28**, 3031 (1983); D. D. Sarma, F. U. Hillebrecht, M. Campagna, C. Carbone, J. Nogami, I. Lindau, T. W. Barbee, L. Braicovich, I. Abbati, and B. De Michelis, Z. Phys. B (to be published).

[3]A. Franciosi and J. H. Weaver, Surf. Sci. **132**, 324 (1983).

[4]P. S. Ho, P. E. Schmid, and H. Foth, Phys. Rev. Lett. **46**, 782 (1981).

[5]O. Bisi and C. Calandra, J. Phys. C **14**, 5479 (1981).

[6]M. Benfatto, A. Bianconi, I. Davoli, L. Incoccia, S. Mobilio, and S. Stizza, Solid State Commun. **46**, 367 (1983).

[7]J. E. Müller, O. Jepsen, O. K. Andersen, J. W. Wilkins, Phys. Rev. Lett. **40**, 720 (1978); J. E. Müller, O. Jepsen, and J. W. Wilkins, Solid State Commun. **42**, 365 (1982).

[8]J. E. Müller and J. W. Wilkins, Phys. Rev. B **29**, 4331 (1984).

[9]F. Smulowicz and D. M. Pease, Phys. Rev. B **17**, 3341 (1978).

[10]P. J. Durham, J. B. Pendry, and C. H. Hodges, Solid State Commun. **38**, 159 (1981).

[11]P. A. Lee, P. H. Citrin, P. Eisenberger, and B. M. Kincaid, Rev. Mod. Phys. **53**, 769 (1981), and references therein.

[12]J. Stöhr and R. Jaeger, J. Vac. Sci. Technol. **21**, 619 (1982).

[13]G. Rossi, R. Jaeger, J. Stöhr, T. Kendelewicz, and I. Lindau, Phys. Rev. B **27**, 5154 (1983).

[14]A. Franciosi, J. H. Weaver, Phys. Rev. B **27**, 3554 (1983), and references therein.

[15]G. D. Mahan, in Solid State Physics, edited by H. Ehrenreich, F. Seitz, and D. Turnbull (Academic, New York, 1974), Vol. 29, p. 75; G. D. Mahan, Phys. Rev. B **11**, 4814 (1975).

[16]P. Nozieres and C. T. De Dominicis, Phys. Rev. **178**, 1097 (1969).

[17]P. H. Citrin, G. K. Wertheim, and M. Schlüter, Phys. Rev. B **20**, 3067 (1979).

[18]M. G. Mason, Phys. Rev. B **27**, 748 (1983).

[19]S. Mobilio, F. Comin, and L. Incoccia (unpublished).

[20]A. Balzarotti, M. De Crescenzi, and L. Incoccia, Phys. Rev. B **25**, 6349 (1982).

[21]S. Valeri, U. Del Pennino, P. Sassaroli, and G. Ottaviani, Phys. Rev. B **28**, 4277 (1983).

[22]V. Bermudez, Appl. Surf. Sci. **17**, 12 (1983), and references therein.

[23]D. E. Sayers, E. A. Stern, and F. W. Lytle, Phys. Rev. Lett. **27**, 1204 (1971).

[24]B. K. Teo and P. A. Lee, J. Am. Chem. Soc. **101**, 2815 (1979).

[25]J. J. Rehr, E. A. Stern, R. L. Martin, and E. R. Davidson, Phys. Rev. B **17**, 560 (1978); E. A. Stern, B. A. Bunker, and S. M. Heald, Phys. Rev. B **21**, 5521 (1980).

[26]P. Rabe, G. Tolkiehn, and A. Werner, J. Phys. C **12**, 899 (1979).

[27]Note that the superposition between EXAFS oscillations above the L_2 and L_3 edges is present only in Pd. In Pd silicides, instead, the L_3 EXAFS signal is less extended and does not affect the L_2 EXAFS analysis.

[28]G. Materlik, J. E. Müller and J. W. Wilkins, Phys. Rev. Lett. **50**, 267 (1983).

[29]Actually, some discrepancies were found: All the features of the measured spectra are reproduced in the calculated spectra, but the high-energy part of the theoretical spectrum lies at lower energies than the measured one. Theses differences were attributed to the omission of the electron-core-hole interaction in the final state (Ref. 28).

[30]B. Aronsson and A. Nylund, Acta Chem. Scand. **14**, 1011 (1960).

[31]The environment built around the Pd central atom is: First shell of Si atoms: $N_1=2$; $R_1=2.39$ Å. Second shell of Si atoms: $N_2=2$; $R_2=2.45$ Å. Third shell of Si atoms: $N_3=5$; $R_3=2.62$ Å. Fourth shell of Pd atoms: $N_4=4$; $R_4=2.78$ Å. Fifth shell of Pd atoms: $N_5=10$; $R_5=2.87$ Å. The Pd shells have inequivalent Pd atoms but their Pd-Pd distance is the same.

[32]Similar values for the S_0^2 factor were also used for reproducing the EXAFS structures of metallic glasses ($Fe_{80}B_{20}$ and $Fe_{80}P_{20}$) since only the Debye-Waller factors could not account for the intensity of the Fe-Fe peak in the radial distribution function [G. S. Cargill III, in *EXAFS and Near-edge Structure, Frascati 1982,* Vol. 27 of *Springer Series in Chemical Physics* edited by A. Bianconi, L. Incoccio, S. Stipcich (Springer, New York, 1983), p. 277]. The complex crystal structure of Pd_2Si and the first-nearest Si cage of Pd may explain the similar findings which, in turn, cannot be only due to static and dynamic disorder.

[33]C. Noguera and D. Spanjaard, J. Phys. F **11**, 1133 (1981). They interpret the K-edge EXAFS spectra of Al and Al_2O_3 by Fontaine *et al.*, J. Phys. F **9**, 2143 (1979), by introducing the screening of the K hole by the conducting electrons. It turns out that the potential as well as the phase shift experienced by the photoelectron inside the central atom are both modified with respect to the ioniclike treatment (Ref. 34).

[34]Within the equivalent core approximation,[24] the core electrons are thought to rearrange themselves around the deep hole in such a way that an ionic $(Z+1)$ potential is experienced by the photoelectron in an EXAFS experiment.

[35]L. A. Grunes, Phys. Rev. B **27**, 2111 (1983).

[36]C. Calandra, O. Bisi, and G. Ottaviani, Surf. Sci. Rep. (to be published). The article reviews recent experimental and theoretical work on the electronic properties of transition metal silicides.

[37]D. N. Pease, G. H. Hayes, M. Choi, J. Z. Budnick, W. A. Hines, R. Hasegawa, and S. H. Heald, in *Proceedings of the Fifth International Conference on Liquid and Amorphous Metals, Los Angeles, 1984* [J. Non-Cryst. Solids **61 & 62**, 1359 (1984)].

[38]E. Belin, C. Bonnelle, J. Flechon, and F. Machizand, J. Non-Cryst. Solids **41**, 219 (1980).

[39]I. Davoli, S. Stizza, A. Bianconi, M. Benfatto, C. Furlani, and V. Sessa, Solid State Commun. **48**, 475 (1983).

[40]J. D. Riley, L. Ley, J. Azoulay, and K. Terakura, Phys. Rev. B **20**, 776 (1979).

[41]B. G. Bagley and F. J. Di Savo, in *Amorphous Magnetism,* edited by H. O. Hooper and A. M. DeGraaf (Plenum, New York, 1973), p. 143; W. A. Hines, L. T. Kabaroff, R. Hasegowa, and P. Duwez, in *Amorphous Magnetism,* edited by R. A. Levy and R. Hasegowa (Plenum, New York, 1977), p. 207.

[42]B. Golding, B. G. Bagley, and F. S. L. Hsu, Phys. Rev. Lett. **29**, 68 (1972).

[43]The α_0 threshold exponent appears to be larger than any reported value, including those of the alkali metals. At present there is no explanation for that, but a refinement of the theoretical x-ray absorption coefficient for alkali metals by MND could be necessary in the case of Pd silicides. Detailed and devoted calculations could shine more light on the physical mechanism of the excitonic Pd $L_{2,3}$ white line in Pd_2Si.

[44]M. De Crescenzi and M. Ghedini (unpublished).

[45]Theoretical calculations are in progress [O. Bisi (private communication)].

[46]F. Comin, J. E. Rowe, and P. H. Citrin, Phys. Rev. Lett. **51**, 2402 (1983).